3362–3370 *Nucleic Acids Research, 1997, Vol. 25, No. 16*

RNA–protein interactions within the 3′ untranslated region of vimentin mRNA

Zendra E. Zehner*, Rebecca K. Shepherd, Joanna Gabryszuk[1], Tzu-Fun Fu, May Al-Ali and W. Michael Holmes[1]

Department of Biochemistry and Molecular Biophysics, Box 980614 and [1]Department of Microbiology and Immunology and The Massey Cancer Center, Medical College of Virginia, Virginia Commonwealth University, Richmond, VA 23298-0614, USA

Received January 24, 1997; Revised and Accepted June 20, 1997

ABSTRACT

Several functions have been attributed to protein binding within the 3′ untranslated region (3′UTR) of mRNA, including mRNA localization, stability, and translational repression. Vimentin is an intermediate filament protein whose 3′ untranslated sequence is highly conserved between species. In order to identify sequences that might play a role in vimentin mRNA function, we synthesized ^{32}P-labeled RNA from different regions of vimentin's 3′UTR and assayed for protein binding with HeLa extracts using band shift assays. Sequences required for binding are contained within a region 61–114 nucleotides downstream of the stop codon, a region which is highly conserved from *Xenopus* to man. As judged by competition assays, binding is specific. Solution probing studies of ^{32}P-labeled RNA with various nucleases and lead support a complex stem and loop structure for this region. Finally, UV cross-linking of the RNA–protein complex identifies an RNA binding protein of 46 kDa. Fractionation of a HeLa extract on a sizing column suggests that in addition to the 46 kDa protein, larger complexes containing additional protein(s) can be identified. Vimentin mRNA has been shown to be localized to the perinuclear region of the cytoplasm, possibly at sites of intermediate filament assembly. To date, all sequences required for localization of various mRNAs have been confined to the 3′UTR. Therefore, we hypothesize that this region and associated protein(s) might be important for vimentin mRNA function such as in localization.

INTRODUCTION

The importance of the mRNA 3′ untranslated region (3′UTR) as a repository for signals determining mRNA processing, polyadenylation, export, stability, localization, translation and cell cycle regulation has become apparent (1–5). A summary of this work indicates that critical RNA–protein interactions are involved and a multitude of RNA elements and binding proteins are being identified as additional contributors to gene regulation. A thorough analysis of these complex elements and proteins will be required in order to fully understand cellular regulation.

Although poly(A) RNA is homogeneously distributed throughout the cytoplasm of cells, various cytoskeletal and other mRNAs have been shown to be localized to specific cellular compartments (6–11). For example, β-actin mRNA is localized to the lamellipodia of chick fibroblasts, whereas α-actin and vimentin mRNA are found in a perinuclear configuration (9). In addition, vimentin mRNA is localized to the costameres in myotubes allowed to differentiate in tissue culture (12–14). Because vimentin transcription is down-regulated during myogenesis *in vivo*, it is difficult to assess the physiological importance of this observation, but it does illustrate the possibility that the same mRNA may localize differently in the cytoplasm of different cell types.

To date, all signals required for mRNA localization, whether in *Drosophila* or higher eukaryotes, have been localized to the 3′UTR (6,15). In some cases, these signals can be multiple and quite complex (16–18). When 3′UTR sequences required for β-actin mRNA localization were attached to the β-galactosidase (β-gal) gene, all β-gal synthesis was directed to the lamellipodia (19,20). Furthermore, protein synthesis was not required for mRNA localization (21). Disruption of microtubules had no effect on localization, but microfilaments were required for the correct sorting of actin mRNA (22). Singer coined the term 'zip-code' to identify those sequences which direct mRNAs to particular cellular locations (11,23).

In the case of intermediate filament proteins (IFPs) like vimentin, it is reasonable that mRNAs are localized. IFPs are coiled-coil polymers postulated to contain as many as 32 chains assembled into the 10 nm filament (24–28). Pulse–chase experiments have indicated that the pool of soluble vimentin in the cell is actually the coiled-coil tetramer, an important intermediate in filament assembly (29). In embryonic muscle cells and fibroblasts, over one-half of the newly-synthesized vimentin is found immediately associated with the cytoskeleton (14). These results suggest the possibility that translation and filament polymerization may be linked. In this regard, co-translational assembly may ensure the close proximity of nascent chains for ease of filament polymerization and suggest the importance of vimentin mRNA localization as a prerequisite for optimal filament formation.

Because vimentin and α-actin mRNAs are directed to a different cellular compartment than β-actin, different localization signals and components should be required. Ultimately, we want to search for cellular factors that direct mRNA to the periphery of the nucleus rather than the lamellipodia. Because of the documented

* To whom correspondence should be addressed. Tel: +1 804 828 8753; Fax: +1 804 828 1473; Email: zehner@gems.vcu.edu

importance of the 3′UTR in such cellular functions, we began by examining protein binding within this region of vimentin mRNA. A comparison of vimentin mRNA sequences from *Xenopus* to man exhibits striking sequence homology even within the non-coding 3′UTR (30). To determine protein binding regions, we synthesized ^{32}P-labeled RNA from the entire 3′UTR, as well as from distinct sub-domains. By band shift assays we have defined a protein binding domain and shown that binding is specific. RNA solution probing studies suggest that this region has a well-defined secondary structure. Due to the sequence conservation of this domain across vertebrates, we hypothesize that it may be important for vimentin mRNA function.

MATERIALS AND METHODS

Subcloning of the 3′UTR of human vimentin mRNA

The entire human vimentin 3′UTR and various sub-regions thereof were obtained by PCR using a human vimentin cDNA as the template (a kind gift of D.Bloch and P.Leder, Harvard University, Cambridge, MA). Each of the 5′-primers contained the 2 nucleotides (nt), gc, (to make the *Eco*RI restriction site internal and guarantee maximum enzymatic digestion), an *Eco*RI restriction site (italics), and the T7 promoter sequence (bold) followed by specific primers (capital letters) to the designated regions of the vimentin cDNA. The sequence position designations refer to the number of bases after the stop codon. For example, P#1 (5′-gc*gaattc***taatacgactcactataggg**CACTCAGTGCAGCAATA-3′) begins at base 11 and ends at base 27 downstream of the stop codon. Other 5′-primers contain the same first 28 nt plus vimentin sequence as follows: P#2 (5′-GTTCTTAACAACCGACA-3′) bases 139–156; P#6 (5′-CAAGAATAAAAAAGAAATCC-3′) bases 37–56; and P#7 (5′-CTTAAAGAAACAGCTTTCA-3′) bases 61–79. The 3′-primers contain 2 nt (to ensure complete digestion), plus a *Bam*HI restriction site (italics), followed by the desired 3′ vimentin sequence (in capital letters) as follows: P#3′L (5′-at*ggatcc*GTTTTTCCAAAGATTTATT-3′) bases 302–320; P#3′S (5′-at*ggatcc*AAAGTATTCTAGCACAAGA-3′) bases 208–226; P#8 (5′-cg*ggatcc*GTTAAGAACTAGAGCT-3′) bases 132–147; and P#10 (5′-ct*ggatcc*TATCTTGCGCTCCTG-3′) bases 100–114. The indicated primers were used to construct the following templates: P#1 and P#3′L for transcript 11/320, P#1 and P#3′S for transcript 11/226, P#6 and P#8 for transcript 37/147, P#7 and P#8 for transcript 61/147, P#6 and P#10 for transcript 37/114, and P#2 and P#3′S for transcript 139/226.

PCR reactions used 50 ng of *Eco*RI-linearized template and 1 μg of each primer for 30 cycles. Following PCR, fragments were digested with the restriction enzymes *Eco*RI and *Bam*HI and cloned into similarly digested pUC18. The content of each subclone was verified by DNA sequencing.

Template 81/108 was synthesized by annealing the oligonucleotides P#14 (5′-*attc***taatacgactcactataggg**CACGGAAAGACGTCAAAAAGTCCTCGCG-3′) bases 81–108, and P#15 (5′-gatcCGCGAGGACTTTTTGACGTCTTTCCGTG**ccctatgtgagtcgtatta***g*-3′) bases 108–81, followed by direct cloning into *Eco*RI and *Bam*HI digested pUC18.

Preparation of ^{32}P-labeled RNA transcripts

Plasmids to be transcribed into RNA were first linearized by *Bam*HI digestion. Transcripts 11/137 and 11/73 were made by first digesting the starting template (clone 11/226) with *Mae*I or *Alu*I, respectively, thereby generating run-off transcripts which terminated at the specific internal restriction site. Preparative amounts of T7 polymerase transcripts were prepared from 25–50 μg of template in the presence of transcription buffer (350 mM HEPES pH 7.5, 30 mM $MgCl_2$, 2 mM spermidine and 40 mM dithiothreitol), 40 U of RNasin, 7 mM each of the four NTPs, and 60 U of T7 polymerase (1.5 U/μg) purified as described (31). Following incubation for 2 h at 40°C, the RNA was purified by HPLC on a TSK2000 molecular sieve column. When required for solution probing studies, RNA was end-labeled with [γ-^{32}P]ATP using T4 polynucleotide kinase following 5′-phosphate removal with either bacterial (32,33) or shrimp alkaline phosphatase per manufacturer's directions, and gel purified as described below.

Analytical amounts of RNA were synthesized from 5–10 μg of linearized template and internally labeled by incorporation of either [α-^{32}P]ATP, [α-^{32}P]CTP or [α-^{32}P]UTP in the presence of transcription buffer (40 mM Tris–HCl pH 8.0, 20 mM $MgCl_2$, 1 mM spermidine, 0.1% Triton X-100 and 5 mM dithiothreitol), 60 U of RNasin, 0.25 μM of the labeled nucleotide plus 250 μM of the remaining nucleotides and 24 U of T7 polymerase (1.5 U/μg) for 2–4 h at 40°C. In later RNA synthesis reactions, the transcription buffer was changed to the HEPES-containing buffer noted above for preparative RNA synthesis. For purification, ^{32}P-labeled RNA was heated at 60°C for 4 min prior to loading on either a 6 or 8% polyacrylamide gel (electrophoresis at 1200 V, 40 mA for ~4 h). The band was excised and the RNA removed either by electrophoresis or soaking overnight in Maxam–Gilbert buffer (0.5 M ammonium acetate, 10 mM magnesium acetate, 0.1 M EDTA, and 0.1% SDS). Following ethanol precipitation, the RNA was washed twice with 70% ethanol prior to use.

Preparation of HeLa whole cell and nuclear extracts

HeLa whole cell extract (a postribosomal supernatant) was prepared from HeLa cells as described (34,35). Protein was concentrated by ammonium sulfate precipitation and dialyzed against 50 mM Tris–HCl pH 7.9, 100 mM KCl, 5 mM $MgCl_2$, 1 mM dithiothreitol, 1% Nonidet P-40 and 20% glycerol (v/v), to remove the ammonium sulfate, and stored in aliquots at –70°C. Nuclear extract was prepared as described (35). Protein concentration was determined by the Bradford assay and was 20 μg/μl for the whole cell extract and 35 μg/μl for the nuclear extract.

RNA band shift assays

^{32}P-labeled RNA (4–6 fmol, 50–100 000 d.p.m.) was incubated with 25–40 mM Tris–HCl pH 7.5, 5–20 mM $MgCl_2$, 150 mM KCl and 4–168 μg HeLa whole cell extract or 5 μg nuclear extract in a final volume of 20 μl for 15 min on ice, after which 50 μg of heparin was added for an additional 5 min. Following the addition of 5 μl of 50% (v/v) glycerol (and tracking dye to only the free RNA samples), complexes were resolved on a 5% polyacrylamide gel containing 5% glycerol (ratio of 40:1 acrylamide:bis) in 0.5× Tris-borate buffer (45 mM Tris–HCl pH 8.3, 45 mM borate, 2.5 mM EDTA) at 15–25 mA for 2–4 h at 4°C. Gels were dried and exposed to film with an intensifying screen at –70°C overnight.

Competition band shift assays were done with 4 fmol of ^{32}P-labeled RNA (base 11/226) and 4 μg of whole cell extract (40 000 d.p.m.). This amount of extract was chosen because it yielded 60% of maximal probe binding activity. Either specific, unlabeled RNA (11/226) or non-specific, brome mosaic virus RNA (BMV) (36), were added at 25–200-fold excess at the

beginning of incubation, prior to extract addition. The counts contained in the shifted or free RNA bands were quantified with a Fuji BioImage Analyzer BAS2000 and the percent shifted calculated as the amount of shifted material divided by the sum of free and shifted counts per lane.

Band shift assays were also performed in the presence of specific antibodies to human vimentin (a kind gift from P.Traub, Max Planck Institute, Heidelberg, Germany), desmin (D8281, a rabbit antibody to the chicken gizzard protein purchased from Sigma), glial fibrillary acidic protein (GFAP: G-A-5, a monoclonal antibody purchased from Sigma), actin (two different antibodies; C4, a monoclonal antibody to vertebrate actin from Boehringer Mannheim Biochemicals, and A-2066, a rabbit anti-actin affinity-isolated antibody from Sigma), the histone 3′-end stem–loop binding protein, SLBP (a kind gift from W.Marzluff, University of North Carolina, Chapel Hill, NC), human nucleolar protein, B23 (a kind gift from C.Hutchinson, University of Dundee, Dundee, Scotland), human La protein (a kind gift from J.Keene, Duke University Medical Center, Durham, NC) and hnRNPC (a kind gift from G.Dreyfuss, University of Pennsylvania School of Medicine, Philadelphia, PA). All antibodies purchased from manufacturers or received from the cited individuals were used as recommended. Two sets of assays were conducted. The antibody was added to the protein extract prior to the addition of RNA or it was added after RNA–protein complex formation. Following incubation, complexes were resolved by PAGE as described above. In both cases, no inhibition of band shifting activity was detected.

UV cross-linking of protein and RNA

Incubation of 15 fmol (250 000 d.p.m.) of ^{32}P-labeled RNA (base 11/205 or 226) with 60 μg HeLa whole cell extract was as described above for band shift assays. Following incubation, the samples were exposed to UV light (254 nm, 100 W) at a distance of 5 cm for 10 min on ice. RNA was removed by digestion with 1 U of RNase T_1 at 37°C for 2 h. The resulting ^{32}P-labeled proteins were resolved by 10% SDS–PAGE in the presence of molecular weight markers. The gel was dried and exposed to XAR film with an intensifying screen at –70°C for 3 days.

Northwestern blot

HeLa whole cell or nuclear extract (5.5 μg) was separated by 9% SDS–PAGE. Following electrophoresis, proteins were allowed to re-fold by soaking for 30 min in TNED buffer (10 mM Tris–HCl pH 7.5, 50 mM NaCl, 0.1 mM EDTA and 1 mM dithiothreitol) and then transferred to nitrocellulose by electrophoresis at 75 V for 1 h. The nitrocellulose was pre-hybridized overnight in 5% (w/v) non-fat dry milk, 50 mM Tris–HCl pH 7.5, 50 mM NaCl, 0.1 mM EDTA and 1 mM dithiothreitol. Following a wash with TNED buffer, hybridization with ^{32}P-end-labeled RNA (37/147, 1.33×10^6 d.p.m.) was in TNED buffer for 2.5 h at room temperature with shaking. Following hybridization, the blot was washed three times, 10 min each, with TNED buffer. After drying, autoradiography was as described above for 10 days.

Determination of RNA secondary structure in solution

The T7 transcript (37/147) was prepared and ^{32}P-labeled at the 5′-end as described above. The single-strand nuclease (ChS) was purified from wheat chloroplasts as described (37) and had an activity of 0.17 U/μl. The double-strand RNase, V_1 (0.7 U/μl), and single-strand RNases T_1 (10 U/μl) and U_2 (10 U/μl) were obtained from Pharmacia. An RNA sequence ladder was generated by limited alkaline hydrolysis of ^{32}P-labeled RNA (1×10^5 d.p.m.) in bicarbonate buffer pH 9.2, at 90°C for 6 min in the presence of bulk yeast tRNA (2 μg). To generate an A- or G-specific ladder, a sample of ^{32}P-labeled RNA was incubated with 0.12 U of RNase U_2 or T_1, respectively, for 12 min at 55°C followed by the addition of 2 μg of tRNA. ^{32}P-labeled RNA was incubated separately with 0.2 and 0.4 U of ChS nuclease or 0.01, 0.011, 0.014 and 0.017 U of RNase V_1 for 5 min at room temperature in TMK buffer (20 mM Tris–HCl pH 7.5, 10 mM $MgCl_2$, 100 mM KCl), or 0.1 and 0.3 U of RNase T_1 in TM buffer (50 mM Tris–HCl pH 7.2, 10 mM $MgCl_2$). Reaction mixtures were phenol–chloroform extracted, adjusted to 0.3 M sodium acetate pH 6.0, and ethanol precipitated with 3 vol ethanol. Pellets were centrifuged, air-dried and re-suspended in loading buffer (20 mM sodium citrate pH 5.0, 7 M urea, 1 mM EDTA, 0.025% xylene cyanol and 0.025% bromophenol blue). Samples were separated by 8% PAGE (acrylamide/bisacrylamide ratio of 19:1) containing 8 M urea and 0.5× TBE. Gels were autoradiographed after drying.

For lead cleavage experiments, ^{32}P-end-labeled RNA was supplemented with 4 μg of yeast total tRNA and incubated with 4 and 12 mM lead acetate for 5 min at 20°C in 20 mM HEPES pH 7.5, 5 mM magnesium acetate, 50 mM potassium acetate. Reactions were stopped by the addition of EDTA to a final concentration of 33 mM. Samples were phenol–chloroform extracted, precipitated, re-suspended in loading buffer, and loaded on a gel as described above.

Protein fractionation on a sizing column

HeLa whole cell extract (32 mg) was fractionated on a Superdex 200 column (16 mm × 70 cm) using HPLC at a flow rate of 1 ml/min, and 70 fractions of 2 ml each were collected.

RESULTS

A comparison of vimentin's 3′UTR mRNAs across species

A number of vimentin genes have now been isolated from a wide range of species. In order to find regions of high homology which might correlate with mRNA function, we compared the 3′UTR sequence of vimentin from human to *Xenopus*, beginning 3′ to the stop codon (set at position 1 relative to the human sequence) and extending to the first functional poly(A) site (Fig. 1). As noted previously, considerable homology exists between vimentin genes both in coding and non-coding regions (38,39). In Figure 1, sequences were aligned in order to maximize homology and nucleotides exhibiting at least a 5 out of 7 match across species have been colored. There are many homologous regions. One exceptionally large region (positions 68–115) extends for 47 contiguous bases and displays 68% homology from *Xenopus* to human. This degree of homology is as great as that exhibited within certain coding regions of the vimentin gene. For example, when comparing the chicken sequence of exon 1 (the most divergent domain) to that of hamster, the homology is only 60% (38). However, within exon 6, the most conserved region, the homology increases to 90%. Thus, portions of vimentin's 3′UTR are as conserved as protein coding regions, which suggests a functional role for this region. In order to ultimately investigate this role, we pursued a further analysis of this region.

As a requisite for function, this region may contain binding sites for regulatory proteins. To date, almost all RNA regulatory proteins bind loops, loops and stems, bulges or combinations thereof (40).

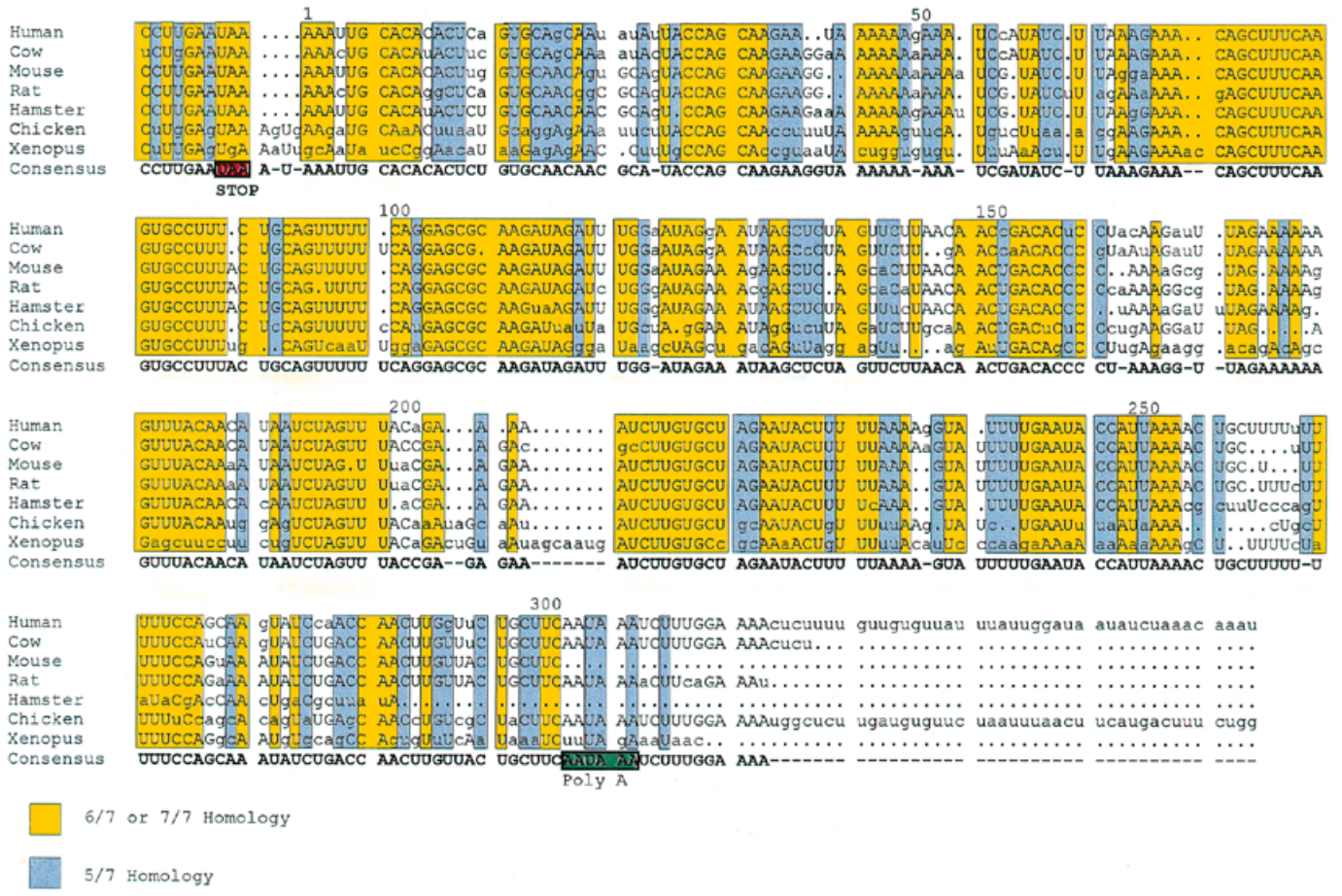

Figure 1. Comparison of the 3′ untranslated sequences of various vimentin mRNAs. Sequences from human (61,62), cow (63), mouse (64), rat (65), hamster (66), chicken (38) and *Xenopus* (39) have been aligned and insertions introduced (.) in order to maximize homology. Nucleotides are numbered based on the human sequence starting at position 1 immediately 3′ to the stop codon and proceeding 300 bases to the functional poly(A) site. A consensus sequence is indicated on the bottom line. Agreement with the consensus sequence is indicated by capital letters. Those positions exhibiting at least 5 out of 7 homology between species are coloured (yellow boxes indicate a 6/7 or better homology; blue boxes 5/7). The stop codon and poly(A) addition sites are labeled. A cryptic poly(A) site, found only in the human sequence, is located at position 41.

Therefore, we analyzed the human vimentin 3′UTR for regions of putative secondary structure (Fig. 2) by applying the computer algorithm of Zucker (41,42). Analysis reveals numerous stem and loop structures, several of which are located within the homologous, colored areas noted above. Interestingly, an extensive secondary structure is observed within the 47 base region (positions 65–115) noted above. However, any of these regions could be protein binding sites, and functional studies were carried out to determine if any of these are actual sites for protein binding.

Localization of a protein binding region within vimentin's 3′UTR

To localize protein binding sites, we synthesized ^{32}P-labeled RNA representing the entire 3′UTR of vimentin, extending from position 11 to 320 nt downstream of the stop codon (11/320), and the same region minus the poly(A) site (11/226). The ability to bind protein was assessed via a band shift assay in the presence of the non-specific competitors, tRNA and heparin. The complete 3′UTR shows considerable protein binding to increasing concentrations of a HeLa whole cell extract (Fig. 3A, lanes 2–4). Although binding of the entire 3′UTR exhibited a broad band of shifted material, removal of the poly(A) site (11/226) resulted in a sharper band, which may be due to the elimination of the poly(A) binding site in the RNA (Fig. 3A, lanes 6–8). Binding occurred over a wide range of KCl concentrations (100–600 mM) with no difference in band shift pattern (data not shown). Also, no difference was detected in the absence of tRNA; therefore, it was removed from subsequent band shift assays.

To determine if binding was specific, the band shift assay was repeated with ^{32}P-labeled RNA (11/226) in the presence of excess specific or non-specific RNA. Here the amount of RNA and extract added was chosen to yield 60% of maximal probe shifting activity. Results were quantified by phospho-image analysis (Fig. 3B). Binding was reduced to 12% in the presence of a 50-fold excess of unlabeled, specific RNA and completely inhibited by an excess of 100-fold. BMV RNA was chosen as a non-specific competitor because it is of comparable length to vimentin (both 215 nt) and has been shown to contain considerable secondary structure (36). The inclusion of up to 200-fold excess of BMV RNA had no significant effect on binding. Therefore, it was concluded that protein binding is specific for vimentin mRNA sequences.

As can be seen in Figure 2, many putative stem and loop structures are possible within vimentin's 3′UTR. To determine which region(s) might be required for binding, various domains

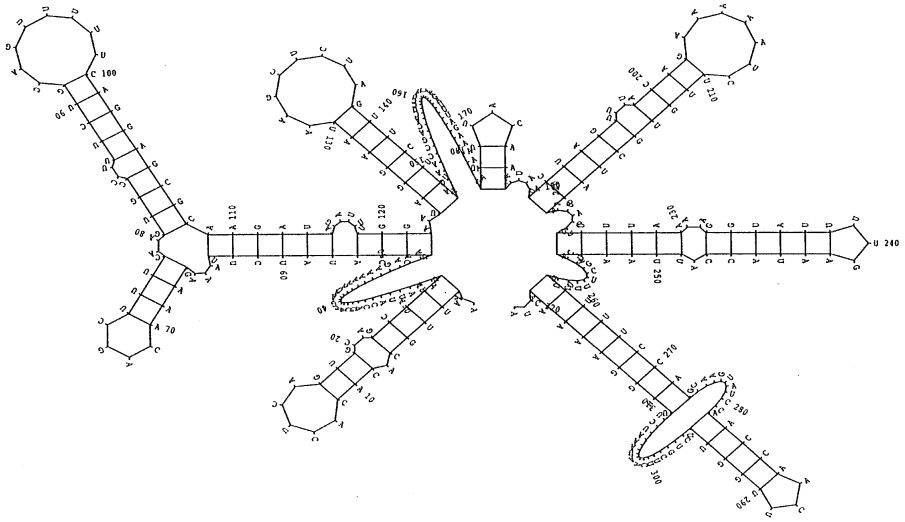

Figure 2. Possible folding of the 3′UTR of human vimentin mRNA. The human vimentin mRNA 3′UTR is folded according to the computer algorithm of Zuker to yield a structure of minimum free energy (41,42).

were subcloned, and ^{32}P-labeled RNA was synthesized. Band shift assays for some of the constructs are shown (Fig. 4A) and the data tabulated (Fig. 4B). As shown previously (Fig. 3), band shift activity occurs with the entire 3′UTR (11/320) and minus the poly(A) site (11/226). Starting from the 5′-end, no shifting occurred with RNA from the minimal region 11–73. However, including sequences up to 137 did result in band shift activity. On the other hand, RNA which began at position 139 and extended to 226 [the 3′-half of vimentin's 3′UTR minus the poly(A) site], did not reveal any band shift activity, although this region could potentially form comparable stems and loops (Fig. 2). RNA containing nucleotides 37/147, 61/147, and 37/114 all exhibited band shift activity (data not shown). Moreover, identical results are found with both HeLa whole cell and nuclear extracts (Fig. 4A, compare lanes 3 and 2 or lanes 8 and 7). In summary, it appears that protein binding is specific to a relatively small region of vimentin's 3′UTR, and a minimal binding domain can be deduced from 61 to 114 nt downstream of the stop codon (Fig. 4B).

It should be noted that although the ^{32}P-labeled RNA is gel purified and exhibits a single band on denaturing polyacrylamide gels run at a high temperature, in some cases several RNA bands are visible in the 'RNA only' lane (Fig. 4A, lanes 1, 4, 6 and 9), as well as in the presence of HeLa extract. These could not be removed by simple re-heating and cooling of the RNA template (data not shown). More importantly, when shifting did occur, all RNA bands shifted equally well (Fig. 4A, compares lanes 5 and 4, or lanes 8 and 7 with lane 6), or not at all if no shifting activity was detectable (Fig. 4A, compare lanes 3 and 2 with lane 1 or lanes 10 and 9). Therefore, it was concluded that these multiple bands are probably different conformers of the same RNA sequence which become evident when non-denaturing gels are run at low temperatures.

Confirmation of secondary structure within vimentin's 3′UTR

We next set out to determine if regions of homology and protein binding display actual secondary structure in solution. As illustrated in Figure 2, sequences which bind protein (residues 61–114) can be folded into prominent stem–loop structures. In order to determine if such structures actually exist in solution, we carried out chemical and enzymatic probing analyses. ^{32}P-end-labeled RNA (37/147) was prepared and cleaved with either ChS, T_1 or V_1 nuclease in order to determine the presence of single- or double-stranded regions. Several such experiments were conducted and a representative gel is shown in Figure 5A. Clear and distinct regions that can be cleaved with V_1 nuclease (double-stranded cuts) are evident in lanes 1–4. Similarly, T_1 and Chs, single-strand-specific cleavage sites, are evident in lanes 5/6 and 7/8, respectively. In addition, ^{32}P-end-labeled RNA was cleaved with molecular lead, which reveals regions that are single-stranded (Fig. 5B). Three regions are distinctly hypersensitive to lead cleavage, (position 62–66, 72–81 and 93–100) and correspond roughly to those delineated with ChS and T_1 cleavage.

Figure 5C summarizes the data for both enzymatic and lead cleavage sites from several such experiments. It can be seen that clearly there is a loop structure encompassing residues 91–100 and 71–74. In addition, there is a major stem structure involving approximately residues 80–91, with complementary sequences 100–108. A bulge in this region as predicted by the folding programs is confirmed by T_1 and Chs cleavages at residues 83, 87, 88, 102 and 103. Overall, the lead cleavage results suggest that sequences 60–68 are probably not in a helical configuration and that a bulged region is evident centered on residues 63–65. Similarly, a non-helical region is evident between residues 76 and 80. Taken together, the above results strongly corroborate the predicted secondary structure.

Characterization of protein(s) which bind vimentin's 3′UTR

The nature of protein(s) binding to vimentin's 3′UTR was investigated by a number of methods. First, the size and number of protein(s) binding were addressed by UV cross-linking of RNA–protein complexes. ^{32}P-labeled RNA (11/205 or 11/226) was cross-linked to protein by exposure to UV light and non-cross-linked RNA removed by digestion with RNase T_1. The resulting ^{32}P-labeled protein was separated by SDS–PAGE in the presence of molecular weight standards (Fig. 6A). For both RNAs, a single band migrating between the molecular weight markers of 34.9 and 53.2 kDa is seen.

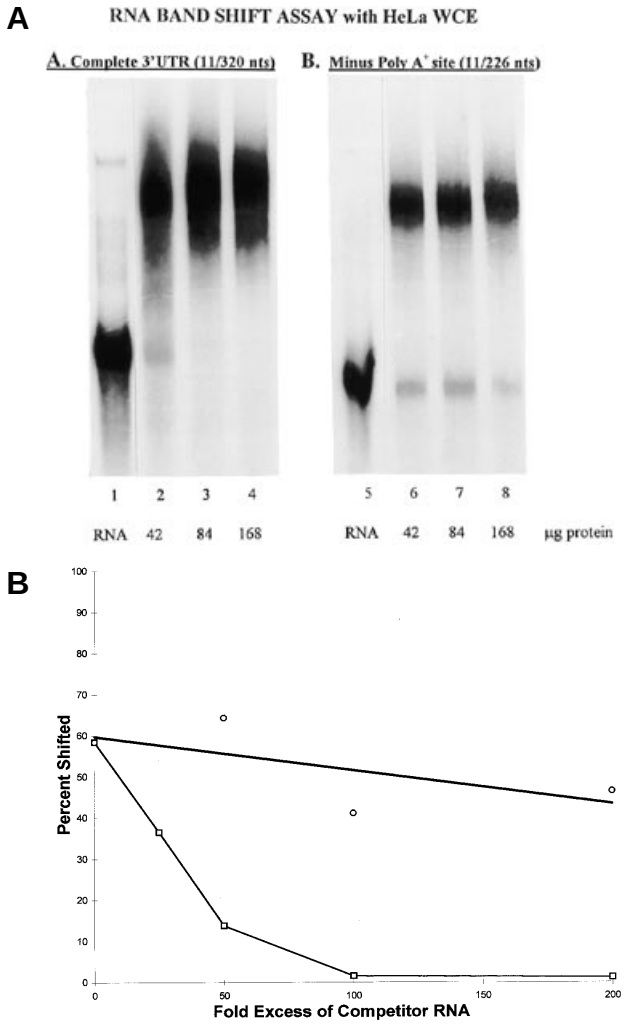

Figure 3. RNA band shift assay with HeLa whole cell extract. (**A**) 6–7 fmol of ^{32}P-labeled RNA from the entire human vimentin 3′UTR (11/320) (lanes 1–4) or minus the poly(A) site (11/226) (lanes 5–8) was incubated alone (lanes 1 and 5, respectively) or with increasing concentrations of HeLa whole cell extract as follows: lanes 2 and 6, 42 µg; lanes 3 and 7, 84 µg; lanes 4 and 8, 168 µg. RNA–protein complexes were separated from free RNA on a 5% polyacrylamide gel, dried and exposed to film overnight at –70°C as described in Materials and Methods. (**B**) 4 fmol of ^{32}P-labeled RNA (11/226) was incubated with 4 µg of HeLa whole cell extract and increasing concentrations (25-, 50-, 100- and 200-fold excess) of the same, specific RNA (□) or non-specific BMV RNA (○). Data was quantified on a BioImage Analyzer and the percent of shifted material is plotted versus the fold-excess of RNA added.

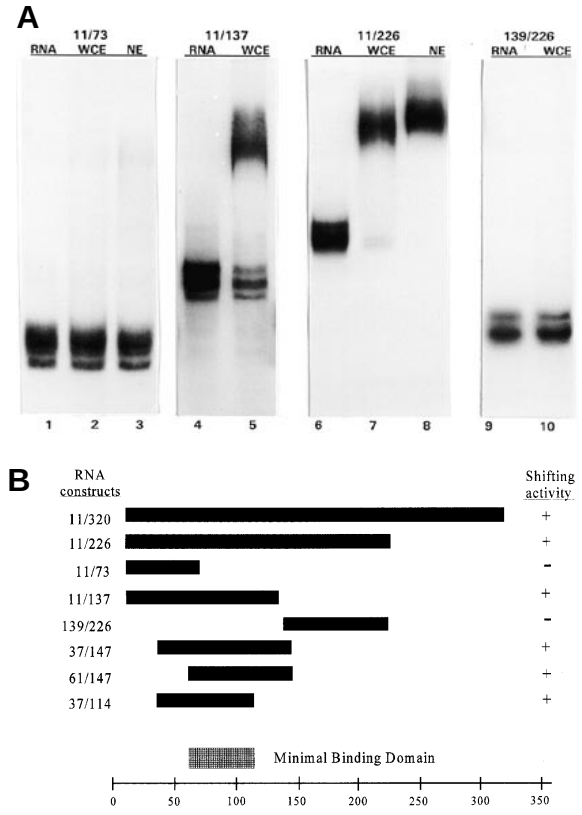

Figure 4. Localization of RNA binding site via band shift assays. (**A**) The ^{32}P-labeled RNA 11/73 (lanes 1–3), 11/137 (lanes 4 and 5), 11/226 (lanes 6–8) or 139/226 (lanes 9 and 10) of human vimentin's 3′UTR was incubated alone (lanes 1, 4, 6 and 9) or with 10 µg HeLa whole cell extract (WCE: lanes 2, 5, 7 and 10) or 5 µg of HeLa nuclear extract (NE: lanes 3 and 8). (**B**) The data from Figure 3A and additional band shift assays not shown are summarized. The deduced minimal binding domain is delineated between 61 and 114 nt downstream of the stop codon.

Second, the size and number of protein(s) binding to vimentin's 3′UTR was assessed by northwestern blot analysis (Fig. 6B). In this case, equivalent amounts of HeLa whole cell and nuclear extract were first separated by SDS–PAGE and the proteins allowed to re-fold before transferring to nitrocellulose. Hybridization with ^{32}P-labeled RNA (37/147) shows a doublet at the position of the 46 kDa molecular weight marker. Interestingly, a faint band is visible at 66 kDa in the nuclear extract (Fig. 6B, lane 2).

Size fractionation of HeLa whole cell extract

It is possible that the 46 kDa RNA binding activity detected in these assays might be part of a larger complex of molecules or contain binding sites for additional polypeptide(s). In order to test this hypothesis, a HeLa whole cell extract was fractionated on a Superdex 200 molecular sieve column and band shift assays with ^{32}P-labeled RNA (37/147) were carried out on the resulting fractions (Fig. 7). Interestingly, activity is detected in two major (lanes 4–6 and lanes 11–14) and a third minor region (lanes 7–10). Relevant fractions were combined as pools I, III and II, respectively. By UV cross-linking the 46 kDa species was found in pool III, which coincides with the position of elution for a 45 kDa molecular weight standard (data not shown). Surprisingly, the largest complex (pool I) which elutes at the position equivalent to 150 kDa, revealed a 66 kDa protein by northwestern blot (data not shown). No binding of the 46 kDa protein could be detected in pool I. In addition, we were unable to detect protein binding by either technique in pool II, eluting at 90 kDa. Perhaps this more minor species is unstable with purification or is refractory to these methods because it requires additional components for binding.

DISCUSSION

An analysis of the 3′UTR from vimentin mRNA across several species (human to *Xenopus*) indicates considerable homology (58% for yellow boxes in Fig. 1), which eclipses that observed for some coding regions (exon 1). By using band shift assays with various ^{32}P-labeled RNAs from the 3′UTR, we have deduced a

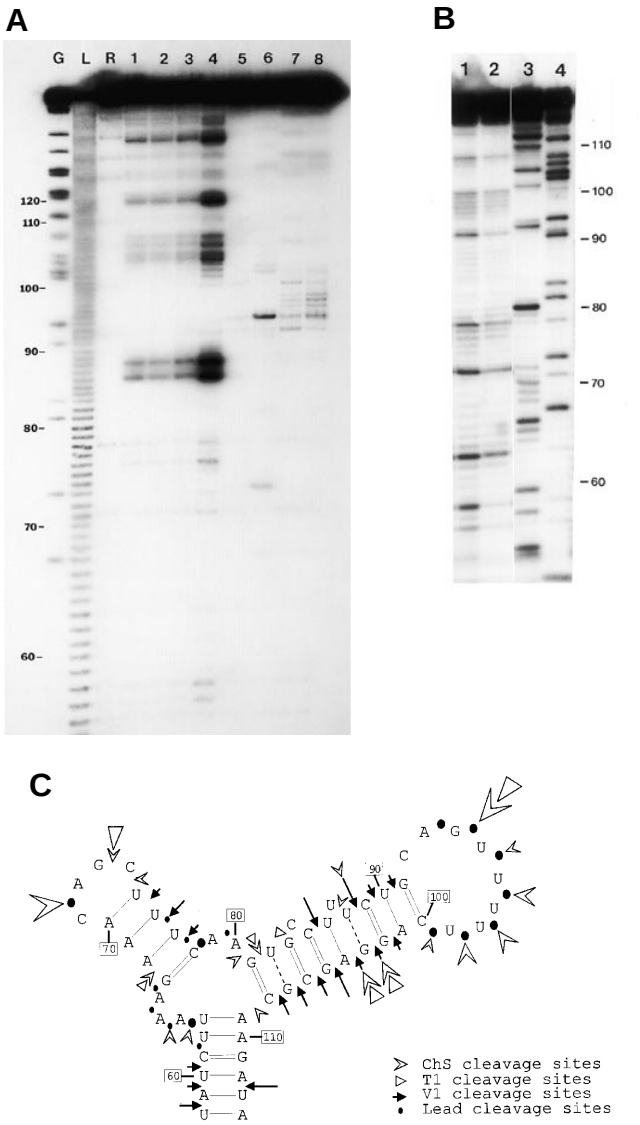

Figure 5. Solution probing of the RNA minimal binding domain with nucleases and lead cleavage. ^{32}P-5′-end-labeled RNA (37/147) of vimentin's 3′UTR is used. (**A**) For reference, the positions of G-specific, RNase T_1 cleavages under denaturating conditions are shown in lane G and an alkaline cleavage ladder is shown in lane L. Uncleaved ^{32}P-labeled RNA is shown in lane R. Cleavage patterns obtained with increasing amounts of the double-strand specific nuclease, V_1, are shown in lanes 1–4, whereas the pattern obtained with the single-strand specific nucleases, RNAse T_1 and Chs, are shown in lanes 5/6 and 7/8, respectively. (**B**) RNase U_2 (A-specific) and T_1 (G-specific) cleavages are shown in lanes 3 and 4, respectively. Cleavage patterns obtained with exposure to 12 or 4 mM lead acetate for 5 min at 20°C are shown in lanes 1 and 2, respectively. For both (A) and (B), fragments were separated on an 8% PAGE sequencing gel as described in Materials and Methods. (**C**) Proposed structure of RNA minimal binding domain as compiled from several experiments. Representative gels are shown in (A) and (B). Bands produced from cleavage with single-strand-specific (ChS or T_1) or double-strand-specific (V_1) nucleases or lead are indicated by the symbols noted on the figure. The size of the icon represents the relative strength of cleavage. Major cleavage points are indicated by the larger symbols and smaller symbols are reserved for the minor cleavage sites.

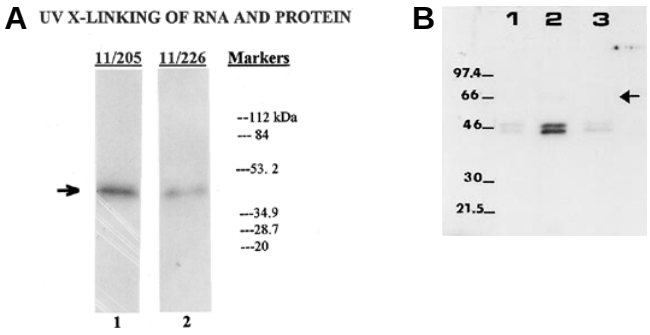

Figure 6. Analyses of RNA binding protein activity. (**A**) UV cross-linking of 15 fmol of ^{32}P-labeled RNA (11/205) and (11/226) of vimentin's 3′UTR to 60 µg of HeLa whole cell extract. Following incubation and UV-irradiation as described in Materials and Methods, non-cross-linked RNA was removed by digestion with RNase T_1 (2 U) for 2 h at 37°C. Protein samples were analyzed on a 10% SDS–PAGE gel, dried and autoradiographed for 3 days at –70°C. The position of migration for several molecular weight markers is as indicated. (**B**) RNA–protein binding was analyzed via a northwestern blot. HeLa whole cell extract (lanes 1 and 3, 5.5 µg) and nuclear extract (lane 2, 5.5 µg) was separated on a 9% SDS–PAGE gel, transferred to nitrocellulose, and incubated with ^{32}P-end-labeled RNA (37/147) (1.33×10^6 d.p.m.) as described in Materials and Methods. The position of migration for several molecular weight markers is indicated. An arrow marks the position of a faint 66 kDa band in lane 2 only.

minimal protein binding domain within the region 61–114 downstream of the stop codon. This minimal binding domain encompasses the 47 base region which exhibits the most extensive homology (68%) from human to *Xenopus*. We have shown that this region in the absence of protein displays a secondary structure in the shape of a 'Y' as deduced from cleavage studies with different nucleases and lead. Interestingly, this Y-shaped region has considerable secondary and possibly tertiary structure, as it contains three stems, two hairpin loops plus a central loop and at least one bulge region. Further application of the Zucker program reveals that similar structures can be drawn for the corresponding region of chicken vimentin mRNA which exhibits band shift activity with HeLa extracts (data not shown). A thorough analysis of what base sequence and structures are required for optimal binding across several species is currently underway. Overall, this region has several general features in common with other known RNA binding domains (5,43–46). Although we have narrowed down the binding site considerably (from 300 to 47 bases), we cannot *a priori* deduce the structure required for protein binding. Additional solution probing studies in the presence of protein(s) will be required to complete this analysis.

RNA–protein interaction appears to be specific for the following reasons. First, band shift assays exhibit competition only with vimentin RNA and not BMV RNA of comparable size and secondary structure. Second, other downstream regions of vimentin's 3′UTR, which potentially contain similar stems and loops, exhibit no binding. Therefore, protein recognition appears to be specific to a particular sequence and/or structure. Third, binding appears to be of appreciable affinity, because it tolerates a wide range of KCl concentrations (data not shown), is stable in heparin, and is independent of the addition of non-specific competitors such as tRNA. In fact, we have found that the addition of 8 M urea is not sufficient to completely obliterate binding.

Several methods have been used to define the size and nature of the protein which binds to vimentin's 3′UTR (Fig. 6). Binding activity is found both in HeLa whole cell as well as nuclear extracts; however, binding is more predominant in nuclear extracts (Fig. 6B). UV cross-linking and northwestern blots show that the major binding protein is 46 kDa, but it may exist in two

forms as suggested by the doublet detected on northwestern blots (Fig. 6B). The lower molecular weight band appears to predominate slightly over the larger species, which suggests that the protein can be modified, perhaps via phosphorylation. Such modification could affect its cellular location and/or binding activity as evidenced by the detection of only a single band on UV cross-linking gels. Finally, fractionation of a HeLa whole cell extract on a sizing column confirms that the shifting activity in pool III corresponds to the position of elution of a 45 kDa protein. Therefore, we conclude from the protein studies that the molecular weight of vimentin's major binding protein is ~46 kDa. We feel it unlikely that this is the β-actin binding protein because in this case a 68 kDa protein was found responsible for mRNA localization to the lamellipodia, a region quite distinct from the proposed perinuclear site for vimentin mRNA (47).

However, when whole cell extract is fractionated on a Superdex 200 column (Fig. 7), three complexes (pools I–III) of different sizes are detected. This could be explained by the interaction of the 46 kDa protein with other peptides, thereby yielding larger complexes. In the case of β-actin, additional proteins of 120, 53 and 25 kDa have been detected which either bind directly to the RNA itself or to the 68 kDa protein (47). In order to address this hypothesis for vimentin mRNA, we analyzed the protein content of the pools by UV-cross-linking and northwestern blots (data not shown). Our initial results confirm the presence of the 46 kDa protein in pool III, but fail to detect its presence in the largest complex, pool I. Instead, a 66 kDa protein was detected by northwestern blot in pool I only. Interestingly, a 66 kDa protein was also barely detectable on the northwestern blot of nuclear extract (Fig. 6B, lane 2). This low level of detection may suggest that this protein is not very abundant and requires partial purification for maximal activity, has lower affinity for RNA, and/or requires additional proteins for optimal binding. In any event, this result raises the possibility that the RNA binding domain defined here can interact with more than one protein (albeit at different affinities) and that binding to the 46 kDa protein may not be a prerequisite for additional protein interaction as has been seen for the 68 kDa protein and β-actin (47). It is obvious that multiple and complex interactions are possible and this may reflect the various components of the complex 'machine(s)' required for mRNA processing, export, localization and/or translation.

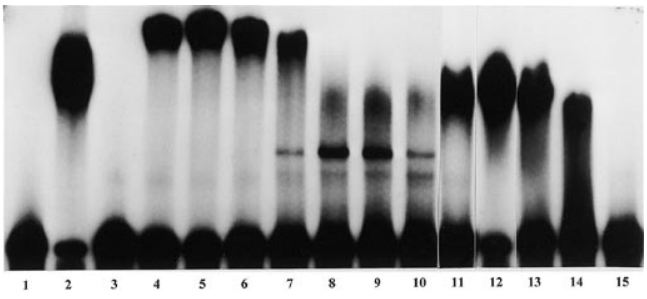

Figure 7. Fractionation of RNA binding activity on a Superdex 200 Column. HeLa whole cell extract (WCE, 32 mg) was fractionated on a Superdex 200 column (16 mm × 70 cm). Starting WCE (lane 2, 20 μg) or 10 μl of each fraction (lanes 3–15, fraction nos 31, 32, 33, 34, 35, 36, 37, 38, 40, 42, 44, 45 and 50) was analyzed by band shift assay with ^{32}P-labeled RNA (37/147) (RNA alone, lane 1) of vimentin's 3′UTR as described in Materials and Methods. Material from fraction nos 31–34, 35–38 and 40–45 were combined into pools I, II and III, respectively. Molecular weight standards of 200, 45 and 12.4 kDa eluted in fractions 31, 42 and 50, respectively.

Having determined the size of the predominant vimentin 3′UTR binding protein, we were interested in establishing its identity. Thus, band shift assays were repeated with antibodies to proteins of the appropriate size and function to be involved in vimentin mRNA regulation. By this method, antibody binding would generate an additional band (a supershift) and thereby identify at least one component of the RNA–protein complex. Because no supershifts were obtained either by adding the antibody prior to RNA protein interaction or following incubation, the data is not shown, and will only be briefly summarized. First, the RNA binding protein is not one of the class III IFP proteins, i.e., vimentin, desmin or GFAP. In view of the auto-regulation of tubulin (48–50), it was a distinct possibility that vimentin could influence its own mRNA localization and/or translation. Secondly, the 46 kDa protein is not actin, although it has been shown that microfilaments are required for mRNA sorting (21). The predominance of the protein in nuclear extracts suggests it could be a member of the hnRNP family; however, antibody to hnRNP C (the family member of comparable size) does not supershift (51). Likewise, antibodies to other known nuclear-localized RNA binding proteins of the appropriate size, B23 or La, do not bind (52–54). A final possibility is SLBP, a 45 kDa protein which binds to the 3′-end of histone mRNA and contributes to cell cycle regulation (5,46). Although vimentin synthesis is also cell-cycle regulated (55,56) and the RNA sequence from position 85 to 105 displays some homology to the SLBP binding site, no binding was evident. Therefore, the identity of this protein is unknown and its purification is underway.

Although the identity of the 46 kDa protein is unknown, its specificity and high affinity for RNA binding suggest a functional role in vimentin mRNA metabolism. Several possibilities exist, such as a role in mRNA splicing, polyadenylation, export, localization, translation, and/or stability, which will be briefly discussed. First, a role in mRNA splicing is unlikely, because there do not appear to be splice sites in vimentin's 3′UTR, or in any of the 3′UTRs for IFP mRNAs isolated to date. Second, a role in polyadenylation is doubtful, because the removal of the poly(A) site does not disrupt binding in the band shift assay, and the minimal binding domain is quite distant (~200 bases upstream) from this site. However, it should be noted that in the human 3′UTR only, there is a cryptic poly(A) site at position 41. Although this site contains a perfectly normal poly(A) consensus sequence (AAUAAA) it does not appear to function *in vivo* (57), probably due to the lack of the additional GU-rich downstream region which is also thought to be required for polyadenylation (58). Such a GU-rich sequence is only found downstream of the functional poly(A) site at position 326. If the cryptic poly(A) site was active, human vimentin mRNA would be synthesized with a short 3′UTR (only 50–60 nt) and would not include the minimal protein binding domain, the consequence of which is unknown. Third, it is unlikely that protein binding is involved in mRNA stability, as vimentin mRNA, along with most other cytoskeletal mRNAs, is reported to be quite stable (59). Furthermore, the well described AU-rich binding site, known to be a stability determinant, is not present within the minimal binding domain. However, it has been found that when a G1-specific, temperature-sensitive, cell cycle mutant is grown at the restricted temperature, vimentin transcripts accumulate in the nucleus and are not transported to the cytoplasm (55,56). The few transcripts that do make it to the

cytoplasm exhibit decreased stability. Moreover, in the case of the neurofilament light gene, the 3′UTR has been found to affect stability (60). These are the only two reported examples of IFP mRNA instability, and for vimentin the more important effect might be in nuclear export rather than mRNA stability.

Overall, we favor the idea that the RNA–protein interaction defined here may be involved in nuclear export, mRNA localization, and/or co-translational assembly of filaments. A role in nuclear export would be suggested by the studies with the G1-specific, mutant cell line where even at the permissive temperature there appears to be a lag of several hours between the peak of vimentin transcriptional activity and the appearance of vimentin mRNA in the cytoplasm (55,56). In addition, we find a predominance of the 46 kDa protein in nuclear extracts. On the other hand, numerous studies support the importance of the 3′UTR in localization (11,19,20,23) and vimentin mRNA has been shown to exhibit a perinuclear localization (9,12–14). Pulse–chase studies demonstrate that co-translational assembly is a strong possibility for vimentin synthesis (29). Therefore, we support any of these latter suggestions as possible roles for the RNA–protein interaction we have detected here. Currently, we are involved in studies to address these hypotheses and hope to elucidate the mechanism of the machine which moves vimentin mRNA from the nucleus to the cytoplasm for subsequent localization and translation.

ACKNOWLEDGEMENTS

The authors wish to acknowledge the advice and encouragement of Drs Chantal and Bernard Ehresmann, Eric Westhof, Alain Krol and Richard Geige at the IBMC and Dr Irwin Davidson at IGBMC, CNRS, Strasbourg, France where this work was initiated by Z.E.Z. and W.M.H. while on sabbatical leave. Also, we wish to acknowledge the computer assistance of Mr Ian Joyce. This work was supported by United States Public Health Service Grant HL-45422 and American Cancer Society Scholar Research Award (to Z.E.Z.), a United States Public Health Service Postdoctoral Training Grant, 5 T32 H107110 (to R.K.S.) and a Poste Rouge from the CNRS, France (to W.M.H.).

REFERENCES

1 Jackson,R.J. (1993) *Cell*, **74**, 9–14.
2 Decker,C.J. and Parker,R. (1995) *Curr. Opin. Cell Biol.*, **7**, 386–392.
3 McCarthy,J.E.G. and Kollmus,H. (1995) *Trends Biochem. Sci.*, **20**, 191–197.
4 Keller,W. (1995) *Cell*, **81**, 829–832.
5 Hanson,R.J., Sun,J., Willis,D.G. and Marzluff,W.F. (1996) *Biochemistry*, **35**, 2146–2156.
6 Wilhelm,J.E. and Vale,R.D. (1993) *J. Cell Biol.*, **123**, 269–274.
7 St. Johnston,D. (1995) *Cell*, **81**, 161–170.
8 Wilson,I.A., Brindle,K.M. and Fulton,A.M. (1995) *Biochem. J.*, **308**, 599–605.
9 Lawrence,J.B. and Singer,R.H. (1986) *Cell*, **45**, 407–415.
10 Singer,R.H. (1992) *Curr. Opin. Cell Biol.*, **4**, 15–19.
11 Kislauskis,E.H. and Singer,R.H. (1992) *Curr. Opin. Cell Biol.*, **4**, 975–978.
12 Morris,E.J. and Fulton,A.B. (1994) *J. Cell Sci.* **107**, 377–386.
13 Fulton,A.B. (1993) *J. Cell Biochem.* **52**, 148–152.
14 Cripe,L., Morris,E. and Fulton,A.B. (1993) *Proc. Natl. Acad. Sci. USA*, **90**, 2724–2728.
15 Gottlieb,E. (1992) *Proc. Natl. Acad. Sci. USA*, **89**, 7164–7168.
16 Gavis,E.R. and Lehmann,R. (1992) *Cell*, **71**, 301–313.
17 Rongo,C., Gavis,E.R. and Lehmann,R. (1995) *Development*, **121**, 2737–2746.
18 Gavis,E.R. and Lehmann,R. (1994) *Nature*, **369**, 315–318.
19 Kislauskis,E.H., Li,Z., Singer,R.H. and Taneja,K.L. (1993) *J. Cell Biol.*, **123**, 165–172.
20 Kislauskis,E.H., Zhu,X. and Singer,R.H. (1994) *J. Cell Biol.*, **127**, 441–451.
21 Sundell,C.L. and Singer,R.H. (1990) *J. Cell Biol.*, **111**, 2397–2403.
22 Sundell,C.L. and Singer,R.H. (1991) *Science*, **253**, 1275–1277.
23 Singer,R.H. (1993) *Curr. Biol.*, **3**, 719–721.
24 Steinert,P.M. and Parry,D.A. (1985) *Annu. Rev. Cell Biol.*, **1**, 41–65.
25 Steinert,P.M. and Roop,D.R. (1988) *Annu. Rev. Biochem.*, **57**, 593–625.
26 Steinert,P.M., Steven,A.C. and Roop,D.R. (1985) *Cell*, **42**, 411–420.
27 Steinert,P.M. and Liem,R.K. (1990) *Cell*, **60**, 521–523.
28 Parry,D.A. and Steinert,P.M. (1992) *Curr. Opin. Cell Biol.*, **4**, 94–98.
29 Soellner,P., Quinlan,R.A. and Franke,W.W. (1985) *Proc. Natl. Acad. Sci. USA*, **82**, 7929–7933.
30 Hesketh,J. (1991) *Biochem. Soc. Trans.*, **19**, 1103–1107.
31 Grodberg,J. and Dunn,J.J. (1988) *J. Bacteriol.*, **170**, 1245–1253.
32 Keith,G., Pixa,G., Fix,C. and Dirheimer,G. (1983) *Biochimie*, **65**, 661–672.
33 Keith,G. (1990) In Gehrke,C.W. and Kuo,K.C. (eds) *Chromatography and Modifications of Nucleosides, Chromatography Library Series*. Elsevier, Amsterdam, pp. A103–A141.
34 Dignam,J.D., Martin,P.L., Shastry,B.S. and Roeder,R.G. (1990) *Methods Enzymol.*, **182**, 194–203.
35 Dignam,J.D., Lebowitz,R.M. and Roeder,R.G. (1983) *Nucleic Acids Res.*, **11**, 1475–1489.
36 Felden,B., Florentz,C., Giege,R. and Westhof,E. (1994) *J. Mol. Biol.*, **235**, 508–531.
37 Monko,M., Kuligowska,E. and Szarkowski,J.W. (1994) *Phytochemistry*, **37**, 301–305.
38 Zehner,Z.E., Li,Y., Roe,B.A., Paterson,B.M. and Sax,C.M. (1987) *J. Biol. Chem.*, **262**, 8112–8120.
39 Herrmann,H., Fouquet,B. and Franke,W.W. (1989) *Development*, **105**, 279–298.
40 Varani,G. and Pardi,A. (1994) In Nagai,K. and Mattaj,I.W. (eds) *RNA–Protein Interactions*. Oxford University Press, Inc., New York, pp. 1–20.
41 Jaeger,A.J., Turner,D.H. and Zuker,M. (1989) *Proc. Natl. Acad. Sci. USA*, **86**, 7706–7710.
42 Zuker,M. (1989) *Science*, **244**, 48–52.
43 Karn,J., Gait,M.J., Churcher,M.J., Mann,D.A., Mikaelian,I. and Pritchard,C. (1994) In Nagai,K. and Mattaj,I.W. (eds) *RNA–Protein Interactions*. Oxford University Press, Inc., New York, pp. 192–220.
44 Pieler,T. (1994) In Nagai,K. and Mattaj,I.W. (eds) *RNA–Protein Interactions*. Oxford University Press, Inc., New York, pp. 178–191.
45 Draper,D.E. (1994) In Nagai,K. and Mattaj,I.W. (eds) *RNA–Protein Interactions*. Oxford University Press, Inc., New York, pp. 82–102.
46 Dominski,Z., Sumerel,J., Hanson,R.J. and Marzluff,W.F. (1995) *RNA*, **1**, 915–923.
47 Ross,A.F., Oleynikov,Y., Kislauskis,E.H., Taneja,K. and Singer,R.H. (1997) *Mol. Cell. Biol.*, **17**, 2158–2165.
48 Gay,D.A., Sisodia,S.S. and Cleveland,D.W. (1989) *Proc. Natl. Acad. Sci. USA*, **86**, 5763–5767.
49 Yen,T.J., Gay,D.A., Pachter,J.S. and Cleveland,D.W. (1988) *Mol. Cell. Biol.*, **8**, 1224–1235.
50 Pachter,J.S., Yen,T.J. and Cleveland,D.W. (1987) *Cell*, **51**, 283–292.
51 Dreyfuss,G., Matunis,M.J., Pinol-Roma,S. and Burd,C.G. (1993) *Annu. Rev. Biochem.*, **62**, 289–321.
52 Borer,R.A., Lehner,C.F., Eppenberger,H.M. and Nigg,A. (1989) *Cell*, **56**, 379–390.
53 Peek,R., Pruijn,G.J. and Van Venrooij,W.J. (1996) *Eur. J. Biochem.*, **236**, 649–655.
54 Svitkin,Y.V., Pause,A. and Sonenberg,N. (1994) *J. Virol.*, **68**, 7001–7007.
55 Hirschhorn,R.R. (1994) *SAAS Bulletin:Biochem. Biotech.*, **7**, 31–35.
56 Ferrier,A.F. and Hirschhorn,R.R. (1997) *J. Cell. Biochem.*, **50**, 245–254.
57 Perreau,J., Lilienbaum,A., Vasseur,M. and Paulin,D. (1988) *Gene*, **62**, 7–16.
58 McDevitt,J.A., Hart,R.P., Wong,W.W. and Nevins,J.R. (1986) *EMBO J.*, **5**, 2907–2913.
59 Ferrier,A.F. and Hirschhorn,R.R. (1992) *J. Cell. Biochem.*, **50**, 245–254.
60 Schwartz,M.L., Bruce,J., Shneidman,P.S. and Schlaepfer,W.W. (1995) *J. Biol. Chem.*, **270**, 26364–26369.
61 Ferrari,S., Battini,R., Kaczmarek,L., Rittling,S., Calabretta,B., de Riel,J.K., Philiponis,V., Wei,J.F. and Baserga,R. (1986) *Mol. Cell. Biol.*, **6**, 3614–3620.
62 Honore,B., Madsen,P., Basse,B., Andersen,A., Walbum,E., Celis,J.E. and Leffers,H. (1990) *Nucleic Acids Res.*, **18**, 6692.
63 Hess,J.F., Casselman,J.T. and FitzGerald,P.G. (1994) *Gene*, **140**, 257–259.
64 Hennekes,H., Kuhn,S. and Traub,P. (1990) *Mol. Gen. Genet.*, **221**, 33–36.
65 Bussemakers,M.J., Verhaegh,G.W., van Bokhoven,A., Debruyne,F.M. and Schalken,J.A. (1992) *Biochem. Biophys. Res. Commun.*, **182**, 1254–1259.
66 Bloemendal,H., Quax,W., Quax-Jeuken,Y., Dodemont,H., Ramaekers,F., Dunia,I. and Benedetti,L. (1983) *Mol. Biol. Rep.*, **9**, 115–118.